ITB formation and MHD activity in experiments with rational surface density control

V.F. Andreev 1), K.A. Razumova 1), I.S. Bel'bas 1), A.Yu. Dnestrovskii 1), A.V. Gorshkov 1), A.Ya. Kislov 1), S.E. Lysenko 1), G.E. Notkin 1), Yu.D. Pavlov 1), V.I. Poznyak 1), D.A. Shelukhin 1), N.N. Timchenko 1), G.W. Spakman 2), M.Yu. Kantor 2)3)4)

1) RRC 'Kurchatov Institute', Institute of Tokamak Physics, 123182 Moscow, Russia
2) FOM-Institute for Plasma Physics Rijnhuizen*, Association EURATOM-FOM, P.O. Box 1207, 3430 BE Nieuwegein, The Netherlands
3) Institute for Energy Research – Plasma Physics*, Forschungszentrum Jülich GmbH, Association EURATOM-FZJ, D-52425 Jülich, Germany
4) Ioffe Institute, RAS, Saint Petersburg 194021, Russia
*Partners in the Trilateral Euregio Cluster

E-mail contact of main author: roma@nfi.kiae.ru

Abstract. In the T-10 tokamak experiments have been conducted for the eITB formation near the rational surfaces, where the magnetic surfaces are rarefied. For this we used off-axis ECR heating for suppression of sawtooth oscillations and the current ramp up. ITB was formed at q=1.5 surface and increases after current ramp-up. As a result, the energy confinement was improved in a factor of 2.5. The limits of self-consistent profiles existence and their destruction by MHD activity are discussed.

1. Introduction

Two main processes determine plasma confinement and the pressure profiles: the self-organized pressure profile and internal/external transport barriers. From previous experiments it is known, that ITBs are formed in the regions, where the turbulent thermal flux is suppressed. i.e. in the regions with very low or zero rational surfaces density [1-3]. In some theoretical papers [4-7] it was argued that the main plasma instabilities develop in the vicinity of rational surfaces and form turbulent cells. These cells are schematically shown in fig. 1. Cells with the various poloidal and toroidal numbers *m*, *n* may overlap, and this may be the reason of the high anomalous thermal transport. It is clear that their possible maximal values *M* and *N* are limited for several reasons: too-long magnetic lines may be destroyed by diffusion processes, the *M* value may be linked to several cells, whose dimensions are of the order of the ion Larmor radius, so at given radius the possible number of cell in poloidal direction has to be limited. The number of modes with *M* and *N* will be different in various parts of the plasma column. Figure 2 shows the results of rational density calculations for M = 20–40 and $N(r) = M(r)/q(r)$.

It has been noted in [4] that in the vicinity of low-order rational surfaces the gaps are located, where modes with *m/n* do not exist. In such gaps the turbulent cells are physically separated, and we have a low transport level as result of such cells location. Estimations, based on this theoretical point of view, gave a value of the heat diffusivity change during the barrier formation, consistent with the experimental one [8].

As has been noted in several papers [3, 9-11], the electron ITBs could be formed in gaps with a low density of rational surfaces, which occur near rational magnetic surfaces with low *m* and *n* numbers, where the gap is widened due to low dq/dr. If this interpretation is valid, we can organize eITB by external impacts in the desirable plasma region. The aim of this report is to study the ITB formation and its properties.

2. T-10 experiments with electron ITB formation

In order to check the role of rational surfaces density in the eITB formation, we carried experiments, which permit us widely vary this value. We used off-axis ECRH (2 gyrotrons with frequency F=130 GHz, P_{ECR}=900 ±50 kW), which suppress sawteeth oscillations, and then rapidly ramp the plasma current with the rate up to 3 MA/s during 15 ms from I_1=160 kA to I_2=206 kA. Note that the wave of additional current density $\Delta j(r)$, calculated by the ASTRA code with Spitzer resistivity ($\eta \sim T_e^{-3/2}$), spreads from the plasma edge to centre with the resistive time ~150 ms.

In shot #56446 with toroidal magnetic field B=2.12 T, off-axis ECRH deposits the power P_{ECR} outside the rational surface q=1 that moves the rational surface q=1 toward the centre. Therefore the distance between rational surfaces q=1 and q=2 is increased. Hence $q(r)$ profile becomes flatten in the vicinity of rational surface q=1.5.

After suppression of sawteeth oscillations, the current rump-up is beginning. In this case, the plasma current density is increased at the edge, and the rational surface q=2 moves outward. Therefore the distance between rational surfaces q=1 and q=2 is increased. So, the $q(r)$ profile becomes very flat in the vicinity of rational surface q=1.5, and the eITB is formed.

It can be expected that after the current ramp-up, the density of rational surfaces is locally changed, leading to increase of gaps in some places, and hence to alleviate the initiation of eITB. The eITB appears in the vicinity of rational surface q=1.5 after off-axis ECRH beginning, and then eITB improves after the current ramp-up. The ASTRA calculation with experimental electron temperature profiles, obtained from Thomson scattering, shows that $q(r)$ profile becomes very flat in plasma core (fig. 3). ASTRA calculation with M<30 shows that near the rational surface q=1.5, the wide gap, the region without rational surfaces appears (fig. 4). Figure 5 shows the temperature time evolution inside (r=13.5 cm) and outside (r=23 cm). Zone with high temperature gradient is seen that confirm the ITB formation.

In some cases, when the electron ITB reaches a high level (ρ^*>0.03, $\rho^* = \rho_s/L_T$, ρ_s is ion Larmor radius for C_s, $L_T = (1/T\, dT/dr)^{-1}$), C_s is an ion sound velocity, the internal disruptions at the rational surface q=1.5 appears (fig. 6). The region of the temperature perturbations lasts 5–6 cm only. They weaken the eITB, but do not destroy it that resembles the ELMy H-mode (fig. 7).

From study of the electron ITB formation we can conclude: 1) we can stimulate the eITB formation by the rational surface density control: 2) sometimes the quality of eITB is limited by the internal disruptions at the rational surface, near which the ITB is formed.

3. Self-organized plasma pressure profile and MHD stability

Many experiments show that the self-consistent normalized pressure profile $p_N(r)$ exists at various tokamaks and in very wide range of operating modes. From these experiments we can conclude [12]:

1) $p_N(r)$ profile is independent on the plasma density and so, on the dominant type of plasma drift wave instability;
2) $p_N(r)$ profile is independent on $j(r)$ profile;
3) the scaling $\rho = r/(I_p R/kB)^{1/2}$ allows us to describe the self-consistent pressure profile $p_N(r)$ for tokamaks with different geometries;

4) the restoration time of self-consistent pressure profile τ_c is less than 0.1 τ_E; where τ_E is the energy confinement time; i.e. τ_c is about the equilibrium establishing time

In order to understand the physical mechanism of pressure profile self-organization, we must find regimes, in which the self-consistent pressure profile is not conserved. In this report we will analyze following three experiments.

3.1. Example 1: electron transport barrier

We know that in the eITB region the gradient of pressure profile is greater than the gradient of self-consistent pressure profile $p_N(r)$. It may be explained in such a way. From results of item 3 we can suppose that the turbulent thermal flux, determined by the turbulent cells overlapping in the vicinity of rational surfaces can be responsible for the conservation of self-consistent pressure profile $p_N(r)$. In a case of electron ITB this turbulent thermal flux is disappeared in ITB region, because the self-consistent pressure profile $p_N(r)$ cannot be sustained in this region. This thermal flux is originated from small-scale turbulence.

3.2. Example 2 – sawteeth oscillations

We know that after sawtooth crush, the self-consistent pressure profile $p_N(r)$ inside the q=1 region is restored during time longer than outside q=1. In fig. 8 the pressure profiles are presented. They were measured at TEXTOR by Thomson scattering in the different time instants in relation to an internal crush. The best self-consistent profile is seen for instants just before the sawtooth crush. Outside q=1 the self-consistent pressure profile $p_N(r)$ exists during sawteeth oscillations.

After each sawteeth crush inside q=1 region the structure of rational surfaces is destroyed and turbulent cells at rational surfaces are destroyed too. So, inside q=1 region, the turbulent flux determined by turbulent cells is disappeared, and the plasma loses the possibility of self-regulation. Later on inside q=1 region the current profile is redistributed and the rational surface structure are restored. In the sequel the turbulent cells are restored too, and plasma obtains the possibility of self-regulation. However, this process is more slower.

As in example 1, we can conclude that the conservation of self-consistence pressure profile $p_N(r)$ is determined by the turbulent flux that formed by turbulent cells overlapping in the vicinity of rational surfaces.

3.3. Example 3 – low q at the plasma boundary

Figure 9(a) show the self-consistent pressure profile $p_N(r)$ for different boundary values of safety factor $q(a)$. All shots with $q(a)\geq 3$ show good conservation of $p_N(r)$, but for $q(a)$=2.2 the pressure profile is steeper than $p_N(r)$. In the latter case there is a high temperature gradient at the plasma boundary owing to strong plasma-wall interaction. It means that the small-scale thermal turbulent flux is not sufficient for regulation of self-consistent pressure profile. Since the small-scale turbulence cannot supply the high thermal flux, then low-number MHD modes should be excited. And indeed, fig. 9(b) shows that such mode is seen during the internal disruption at the rational surface q=2 in discharge with $q(a)$=2.2.

4. Discussion

These experiments permit us to look from another point of view on the processes, leading to a total plasma disruption. When the external impact tries to distort the self-consistent pressure profile $p_N(r)$ too strongly (too low q_{edge}, or too strong gas puffing, cooling periphery, and so on), the small-scale turbulence cannot supply enough thermal flux for conservation of self-consistent pressure profile $p_N(r)$ and low-number MHD modes are excited (at first the mode q=2). Internal disruption with mode q=2 destroys the rational surface structure and turbulent cells in a wide region. So plasma loses its self-organization possibility in this region and it generates development of another MHD modes. Then the next mode q=1 is excited. It destroys the rational surfaces structure and turbulent cells in the plasma core and the total plasma disruption takes place.

Figure 10 illustrates this process step by step. After each crush, the self-consistent pressure profile $p_N(r)$ is not restored totally at the external part of plasma. So, after sequent crush the pressure profile $p_N(r)$ partially destroys (fig. 10(a)). Later the crush consistencies destroyed pressure profile $p_N(r)$ in the plasma core and plasma loses the possibility of self-consistent pressure profile $p_N(r)$ restoration totally. Then mode q=1 is excited and the total plasma disruption takes place (fig. 10(b)).

5. Conclusions

1) The conservation of self-consistent pressure profile $p_N(r)$ is determined by the turbulent thermal flux that formed by turbulent cells overlapping in the vicinity of rational surfaces. This thermal flux is determined by small-scale turbulence.
2) The conservation of self-consistent pressure profile $p_N(r)$ leads to macroscopic MHD plasma stability.
3) Therefore it is not necessary to stabilize different plasma instabilities. We should only provide the conservation of self-consistent pressure profile $p_N(r)$. The principal problem is to arrange the corresponding boundary conditions.
Note that we should take into account self-consistency of pressure profile in simulations of ITER plasma parameters.

References

[1] JOFFRIN, E., et al., Nucl. Fusion **43 (**2003) 1167.
[2] RAZUMOVA, K.A., et al., Nucl. Fusion **44** (2004) 1067.
[3] AUSTIN, M.E., et al., Phys. Plasmas **13 (**2006) 082502.
[4] BEKLEMISHEV, A.D. and HORTON, W., Phys. Fluids B **4 (**1992) 200.
[5] WALTZ, R.E., et al., Phys. Plasmas **13 (**2006) 052301.
[6] KADOMTSEV, B.B., Plasma Phys. Control. Fusion **34 (**1992) 1931.
[7] KISHIMOTO, Y., et al., Nucl. Fusion **40 (**2000) 667.
[8] SHELUKHIN, D.A. et al., Plasma Phys. Rep. **31 (**2005) 985.
[9] RAZUMOVA, K.A., et al., Plasma Phys. Control. Fusion **45 (**2003) 1247.
[10] RAZUMOVA, K.A., et al., Plasma Phys. Control. Fusion **48 (**2006) 1373.
[11] JOFFRIN, E., et al., Nucl. Fusion **43 (**2003) 1167.
[12] RAZUMOVA, K.A., et al., Nucl. Fusion **49** (2009) 065011.

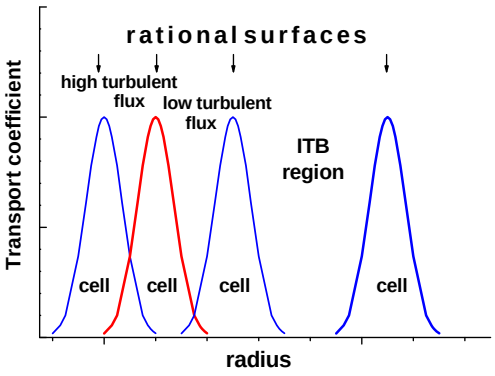

FIG. 1. The scheme of turbulent cells and turbulent flux. The transport level depends on the distance between low- order rational surfaces, the width and the level of turbulent transport inside the cell. When the cell overlapped, the transport is high, gap corresponds to reduced transport (ITB).

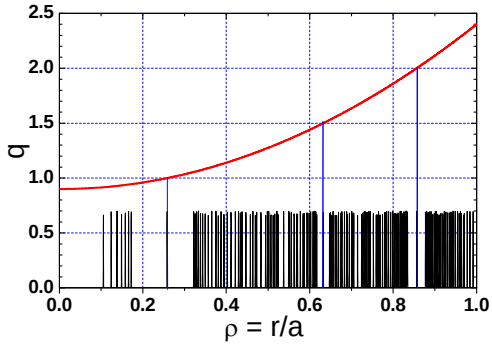

FIG. 2. Positions of rational surfaces with various m/n. Gaps near surfaces with low-order rational q are seen; maximal M = 20–40, maximal N = M/q.

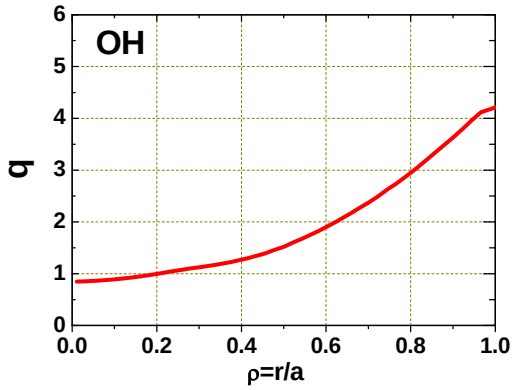

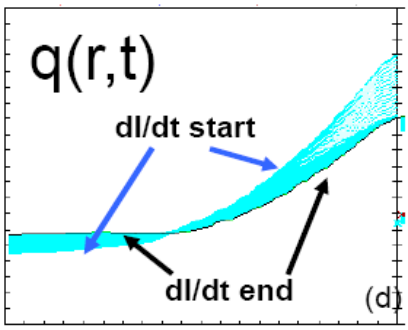

FIG. 3. ASTRA calculation of q(r) profile evolution in shot with current ramp up. a) ohmic stage, b) ECRH plus current ramp up.

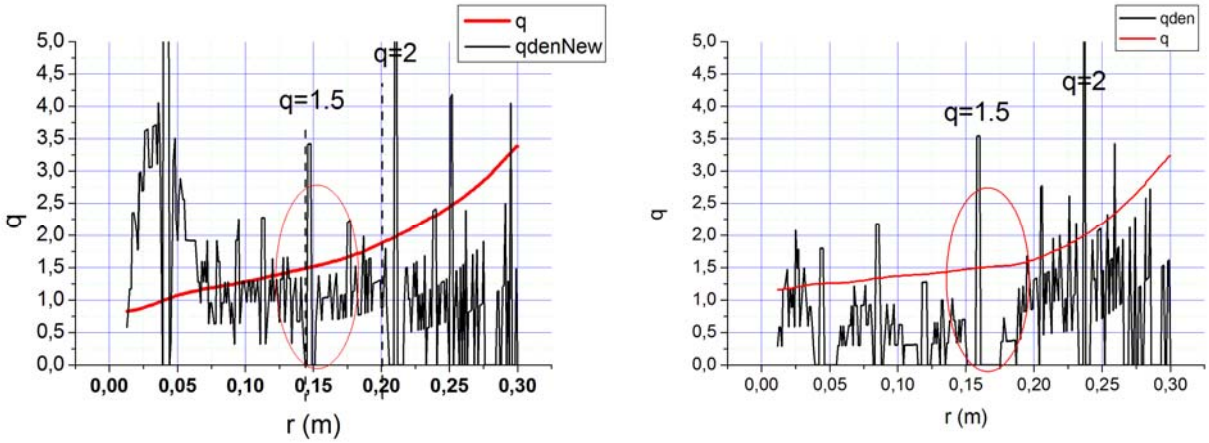

FIG. 4. ASTRA calculation of q(r) profile and the density of rational surfaces at ohmic stage (a) and after off-axis ECRH and current rump-up (b). Gap near q=1.5 is marked by red ellipse.

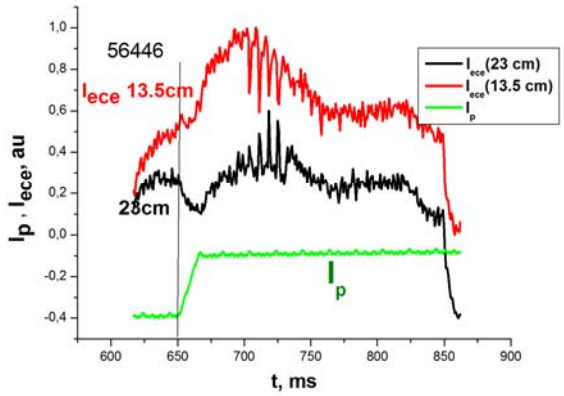

FIG. 5(a). Temperature time evolution inside (r=13.5 cm) and outside (r=23 cm) eITB region.

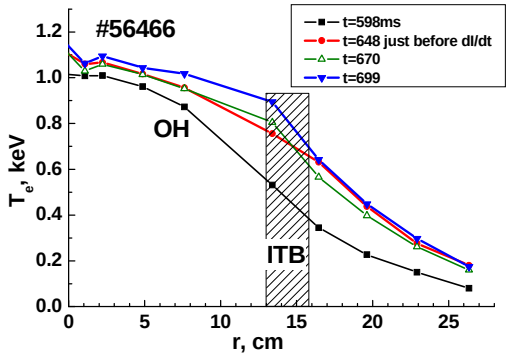

FIG. 5(b). Temperature profiles before (t=648 ms) and after (t=670 ms, t=699 ms) eITB formation.

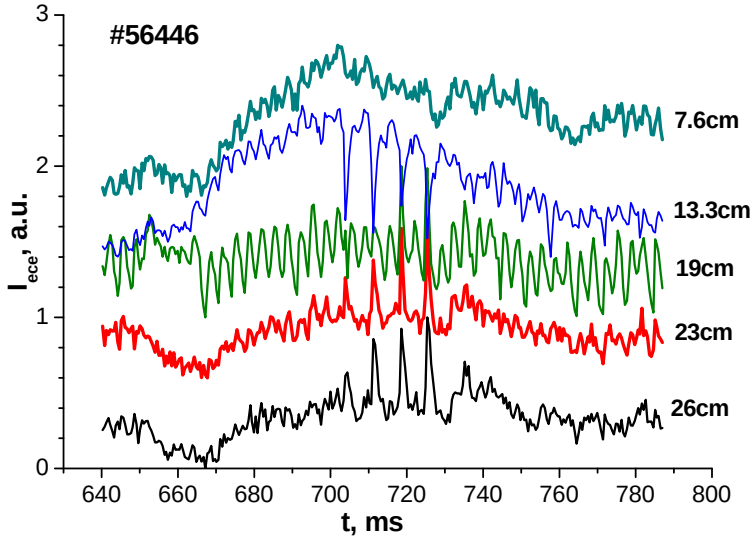

FIG. 6. Time traces of electron temperature for different radii in off-axis ECRH+dI/dt case. Strong ELM-like spikes occur at 710<t<730 ms.

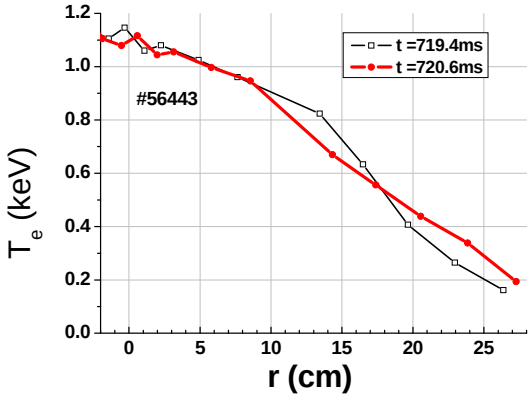

FIG. 7(a). Temperature profiles before (t=719.4 ms) and after (t=720.6 ms) the internal disruption at rational surface q=1.5.

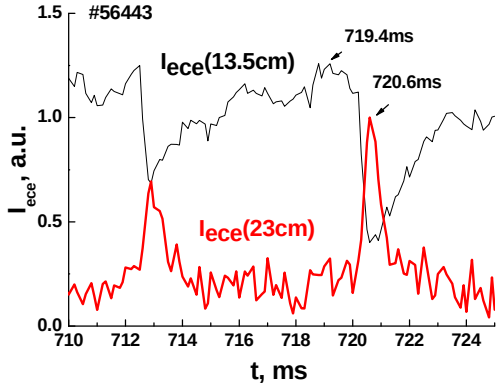

FIG. 7(b). The time evolution of temperature inside (r=13.5 cm) and outside (r=23 cm) the rational surface q=1.5.

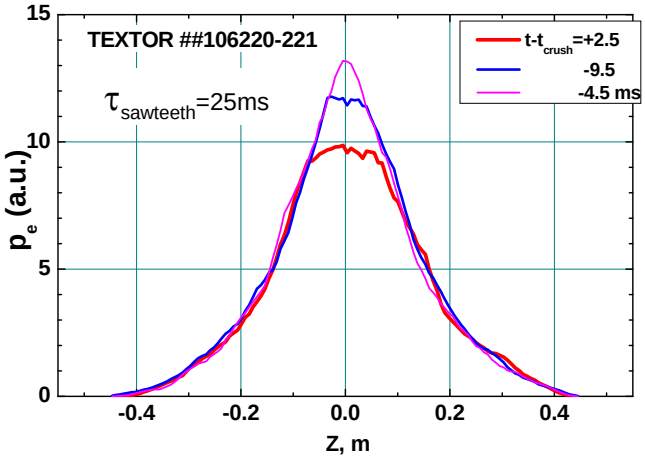

FIG. 8. The pressure profiles for random time instants in relation to internal *crush (TEXTOR, #106220-106221).*

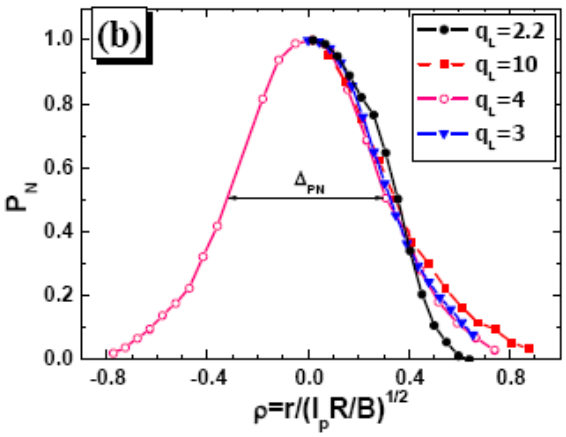

FIG. 9(a). The normalized pressure profiles $p_N(r)$ for different edge safety factor q(a).

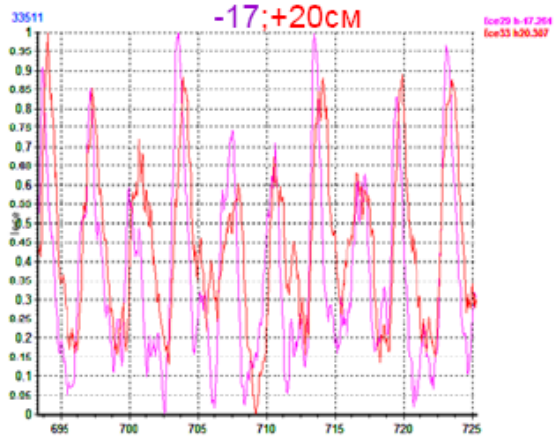

FIG. 9(b). Mode m=2 for case q(a)=2.2 at plasma edge.

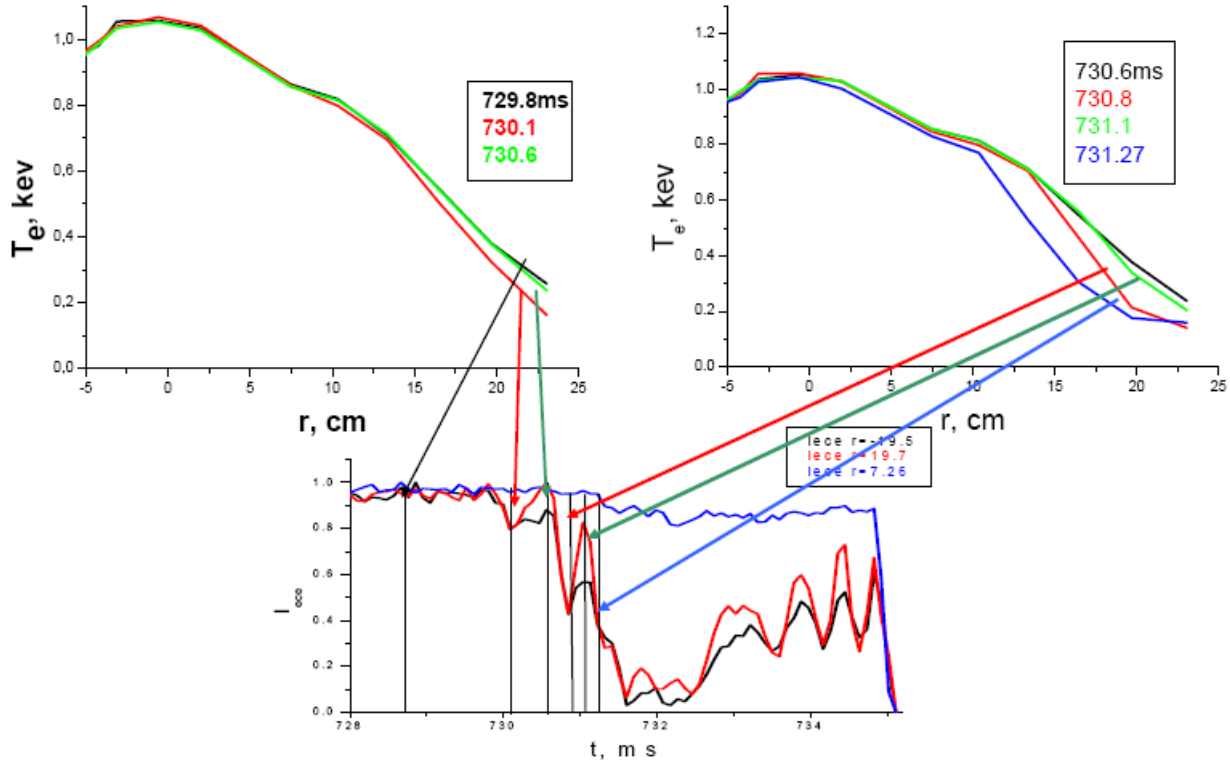

FIG. 10(a). The temperature profile evolution at the mode q=2 crush.

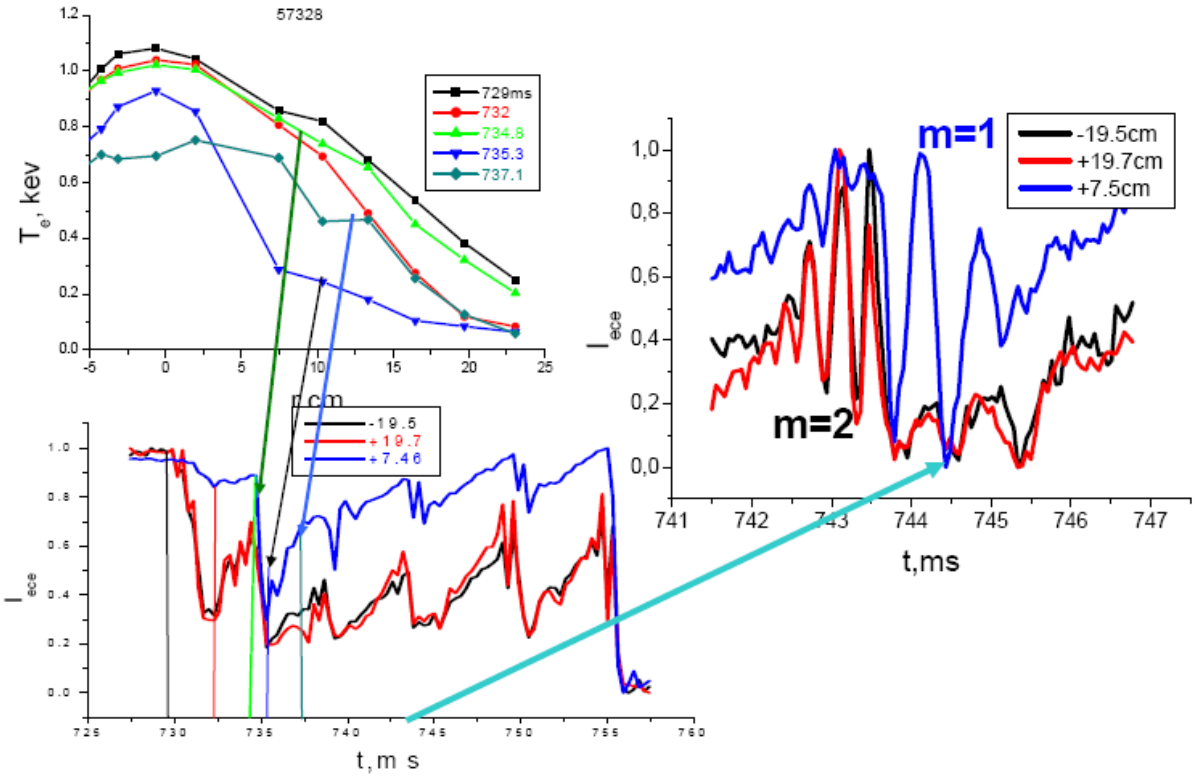

FIG. 10(b). The temperature profile evolution at mode q=2 crush and mode q=1 disruption.